

## Observation of Lasing Mediated by Collective Atomic Recoil

D. Kruse, C. von Cube, C. Zimmermann, and Ph.W. Courteille

*Physikalisches Institut, Eberhard-Karls-Universität Tübingen, Auf der Morgenstelle 14, D-72076 Tübingen, Germany*

(Received 7 May 2003; published 29 October 2003)

We observe the buildup of a frequency-shifted reverse light field in a unidirectionally pumped high- $Q$  optical ring cavity serving as a dipole trap for cold atoms. This effect is enhanced and a steady state is reached, if via an optical molasses an additional friction force is applied to the atoms. We observe the displacement of the atoms accelerated by momentum transfer in the backscattering process and interpret our observations in terms of the collective atomic recoil laser. Numerical simulations are in good agreement with the experimental results.

DOI: 10.1103/PhysRevLett.91.183601

PACS numbers: 42.50.Vk, 34.50.-s, 42.55.-f, 42.60.Lh

Since the first observation of photonic recoil [1], a large variety of techniques has been developed to exploit the mechanical forces of light for optical cooling and trapping. The inverse process, i.e., the impact of the atomic motion on light fields, has recently received special attention with the theoretical prediction [2] and the observation [3,4] of the phenomenon of recoil-induced resonances (RIR) and with the proposal for a collective atomic recoil laser (CARL) [5]. In RIR experiments a pump and a weak probe laser beam having different frequencies give rise to a moving standing light wave at the intersection region. Atoms moving synchronously to this wave undergo two-photon Raman transitions between momentum states. This gives rise to a density grating at the intersection region, which copropagates with the standing wave. The density modulation corresponds to a classical bunching of atoms in the optical potential valleys formed by the standing wave. The Raman scattering process can equivalently be described as stimulated Rayleigh scattering of photons off the density grating [3] from one beam into the other. If the probe laser is red detuned from the pump, it receives a net gain. The probe gain increases the amplitude of the standing wave. This leads to stronger atomic bunching and, in turn, strengthens the Rayleigh scattering in an avalanche process. In RIR experiments the relative gain is typically small, so that runaway amplification of the probe is not observed. Consequently, the positive feedback described above is neglected in common RIR theories.

CARL which shares the same gain mechanism as RIR [6] has been formulated as a transient process [5], the signature of which is an exponential growth of a seeded probe field oriented reversely to a strong pump interacting with an active medium. On the other hand, atomic bunching and probe gain can also arise spontaneously from fluctuations with no seed field applied [7]. The underlying runaway amplification mechanism is particularly strong, if the reverse probe field is recycled by a ring cavity. So far, attempts to observe CARL action have been undertaken only in hot atomic vapors [8,9]. They have led to the identification of a reverse field with some of the expected

characteristics. However, the gain observed in the reverse field can have other sources [10], which are not necessarily related to atomic recoil, so that the unambiguous experimental proof of the CARL effect is still owing.

The CARL effect should emerge most clearly in cold atomic clouds in a collisionless environment [6]. Furthermore, large detunings of the lasers far outside the Doppler-broadened profiles of the atomic resonances are preferable. In this regime effects from atomic polarization gratings, which are not based on density variations [10], are avoided. Finally, to emphasize the role of the exponential gain responsible for self-bunching, i.e., spontaneous formation and growth of a density grating, it is desirable not to seed the probe. The observation of a probe beam is then a clear indication for CARL in contrast to RIR, where the avalanche effect is nonexistent. In this paper we present experiments which fulfill the above requirements.

Our high- $Q$  ring cavity consists of one plane and two curved mirrors. It is 8.5 cm long, has a beam waist of  $w_0 = 130 \mu\text{m}$ , and an amplitude decay rate of  $\kappa = 2\pi \times 22 \text{ kHz}$ . The cavity is pumped by a Ti-sapphire laser. For the sake of definiteness, we describe in the following the cavity modes by their field amplitudes scaled to the field per photon [11]. The mode  $\alpha_+$  is continuously pumped at a rate  $\eta_+ = \sqrt{\delta\kappa}\alpha_+^{(\text{in})}$ , where  $\delta$  is the free spectral range of the cavity and  $\alpha_+^{(\text{in})}$  the field amplitude of the incoupled laser beam. The Ti-sapphire laser is stabilized to this mode by the Pound-Drever-Hall method. The counter-propagating mode is labeled by  $\alpha_-$ . We call  $\alpha_+$  the pump and  $\alpha_-$  the probe mode. The details of the apparatus have been published in Ref. [4]. We load  $^{85}\text{Rb}$  atoms from a magneto-optical trap (MOT) into a  $\text{TEM}_{00}$  mode of the ring cavity. With typically  $N = 10^6$  atoms trapped, we achieve atom peak densities of more than  $2 \times 10^{11} \text{ cm}^{-3}$  at temperatures of several  $100 \mu\text{K}$  corresponding roughly to 1/5 of the potential depth. The temperature of the atomic cloud and its density distribution are monitored by time-of-flight absorption imaging. We measure the intracavity light power via the fields leaking through one of the cavity mirrors (intensity transmission

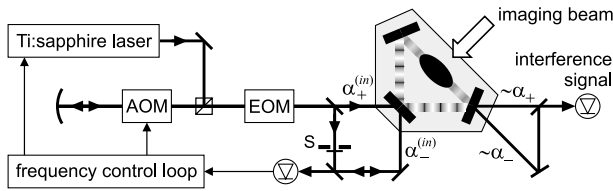


FIG. 1. Scheme of the experimental setup. A Ti-sapphire laser is locked to one of the two counterpropagating modes ( $\alpha_+$ ) of a ring cavity. The beam  $\alpha^{(in)}$  can be switched off by means of a mechanical shutter (S). The atomic cloud is located in the free-space waist of the cavity mode. We observe the evolution of the interference signal between the two light fields leaking through one of the cavity mirrors and the spatial evolution of the atoms via absorption imaging.

$T = 1.8 \times 10^{-6}$ , see Fig. 1). The outcoupled light power is related to the intracavity power by  $P_{\pm}^{(out)} = TP_{\pm}^{(cav)} = T\hbar\omega\delta|\alpha_{\pm}|^2$ . The phase dynamics of the two counterpropagating cavity modes is monitored as the beat signal between the two outcoupled beams. Any frequency difference between pump and probe,  $\Delta\omega \equiv \omega_+ - \omega_-$ , i.e., propagation of the standing wave nodes inside the ring cavity, is translated into an amplitude variation of the observed interference signal  $P_{\text{beat}} = T\hbar\omega\delta|\alpha_+ + \alpha_-|^2$ .

In order to observe a CARL signal, we load atoms from the MOT into the symmetrically pumped ring cavity standing wave ( $\lambda = 797.0$  nm). The detuning from the nearest atomic transition (*D1* line at 794.8 nm) is 1 THz. After 30 ms trapping time one beam ( $\eta_-$ ) is switched off via a mechanical shutter. With no atoms the interference signal  $P_{\text{beat}}$  then drops to  $T\hbar\omega\delta|\alpha_+|^2$  within a time of 10  $\mu\text{s}$ , limited by the finite shutter closing time. An observed residual low-frequency fluctuation of  $P_{\text{beat}}$  is assigned to scattering at the imperfect mirror surfaces. In contrast, if atoms are loaded into the ring cavity standing wave, oscillations appear on the interference signal shortly after the switch-off, as shown in Fig. 2(a). Their amplitude is rapidly damped, however they are still discernible after more than 1.5 ms, which exceeds the cavity decay time  $\tau = (2\kappa)^{-1}$  by more than a factor of 600. We verified that the oscillations do not occur for low cavity finesse, which is realized by rotating the polarization of the incoupled lasers from *s* to *p* polarization [4], thereby reducing the finesse from 80 000 to 2500. Figure 2(c) shows the frequency of the interference signal as a function of time. From the observations we can deduce (i) that the probe mode  $\alpha_-$  is fed with light in the presence of atoms, thus leading to a standing wave superposed to the pump mode  $\alpha_+$ . (ii) Having verified that the oscillations are solely due to a relative phase shift of the cavity modes (no oscillations are detected in either mode), we know that the detuning between probe and pump increases in time, and therefore the standing wave is displaced and accelerated by the presence of atoms. (iii) With time the contrast of the standing wave reduces to zero, i.e., after a

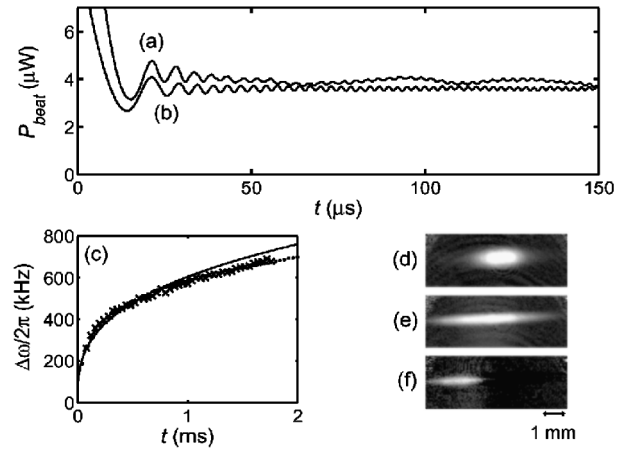


FIG. 2. (a) Recorded time evolution of the observed beat signal between the two cavity modes with  $N = 10^6$  and  $P_{\pm}^{(cav)} = 2$  W. At time  $t = 0$  the pumping of the probe  $\alpha_-$  has been interrupted. (b) Numerical simulation according to Eq. (1) with the temperature adjusted to 200  $\mu\text{K}$ . (c) The symbols ( $\times$ ) trace the evolution of the beat frequency after switch-off. The dotted line is based on a numerical simulation. The solid line is obtained from Eq. (3) with the assumption that the fraction of atoms participating in the coherent dynamics is 1/10 to account for imperfect bunching. (d) Absorption images of a cloud of  $6 \times 10^6$  atoms recorded for high cavity finesse at 0 ms and (e) 6 ms after switching off the probe beam pumping. All images are taken after a 1 ms free expansion time. (f) This image is obtained by subtracting from image (e) an absorption image taken with low cavity finesse 6 ms after switch-off. The intracavity power has been adjusted to the same value as in the high finesse case.

fast initial decay, the probe fades out on a time scale of 1.5 ms. (iv) The atoms are dragged by the moving standing wave. The frequency shift of the backscattered light field by up to 1 MHz corresponds to an atomic velocity of 40 cm/s. At interaction times of a few ms, the atomic motion should lead to a detectable displacement. To verify this we have taken time-of-flight absorption images of the atomic cloud at various times after one-sided switch-off, shown in Figs. 2(d) and 2(e). We observe that, even though a major fraction of the cloud stays at the waist of the laser beam, its center of mass is shifted along the propagation direction of the standing wave. In the case of low cavity finesse, the displacement is almost zero.

The observations can be understood in terms of lasing mediated by collective atomic recoil, despite the differences between our system and the original CARL proposal [5]. The original idea is based on injecting a homogeneously distributed monokinetic atomic beam counterpropagating to the pump and a seed for the probe, which predetermines the probe frequency. In this system, the signature for CARL action is a blue-detuned amplified probe pulse followed by a highly irregular evolution of the system. In contrast, in our system the probe frequency and the atomic momentum distribution evolve in a self-consistent manner. Initially the atoms are highly bunched

at the antinodes of the symmetrically pumped standing wave cavity field. After switching off  $\eta_-$ , those atoms which take part in the CARL process transfer photons from the pump into the probe and by recoil, acquire momentum,  $mv$ , in the direction of the pump. The frequency difference between probe and pump corresponds to twice the Doppler shift,  $\Delta\omega = 2kv$ . Thus, in agreement with our observations, an increasingly red-detuned probe beam is expected, whose intensity eventually diminishes, because its frequency drifts out of the cavity resonance by an amount corresponding to  $\Delta\omega$ .

Being focused on studies of transient phenomena, the original CARL model does not consider relaxation for the translational degrees of freedom. The long-term dynamics predicted by this model yields atomic acceleration without any bounds [12]. To obtain steady-state operation, the addition of dissipation to the momentum equations has been suggested [13,14]. We translate this idea to experiment by introducing a friction force by means of a superimposed optical molasses: In a second set of experiments, we load the atoms from the MOT directly into the unidirectionally pumped running wave dipole trap ( $\eta_- = 0$ ). In contrast to the first set of experiments, we now start from a basically homogeneous atomic density distribution, so that the appearance of light in the probe mode constitutes an evidence for self-bunching. After 40 ms trapping time, we switch on the optical molasses. We use the laser beams of the MOT and tune them 50 MHz below the cooling transition ( $D2, F = 3 \rightarrow F' = 4$ ). Figure 3(a) shows the interference signal observed when the optical molasses is turned on at time  $t = 0$ . Apparently, strong oscillations emerge from the noise floor. They quickly reach a steady frequency between 100 and 170 kHz, which corresponds to an atomic velocity of 7 to 13 cm/s, and they persist for times longer than 100 ms, mainly limited by the finite size of the molasses region. Figure 3(c) demonstrates the dependence of the beat frequency on the pump rate  $\eta_+$ .

We interpret the experimental observations in the following way: Any inhomogeneity in the atomic density distribution, e.g., due to a residual standing wave ratio in the cavity field generated by backscattering from the cavity mirrors, gives rise to some amount of atomic bunching. Without the optical molasses, this bunching is not sufficient to initiate runaway CARL amplification, mainly because the atoms are accelerated and redistributed in space, before a relevant bunching of the atomic density can occur. The damping force of the molasses now counteracts the acceleration force and prevents dispersion of the atomic velocities. A steady-state velocity is reached, when the velocity dependent damping force balances the CARL acceleration. The molasses thus acts like a pump recycling the atoms into an equilibrium momentum state that otherwise would be depleted by CARL acceleration. The equilibrium defines the frequency of the probe, which therefore is dependent on

the intensity of the pump laser, as shown in Fig. 3(c), and the molasses parameters. We found that the frequency also depends on the atom number.

We model our system consisting of an ensemble of atoms coupled to two counterpropagating modes of a ring cavity with a set of differential equations [7,11,15]. We concentrate on the limit of very large laser detuning from the atomic resonances, where the excited atomic states can be adiabatically eliminated [Eqs. (16)–(18) in Ref. [11]]. Adapting this model to our experiment, we have to account for the fact that one mode, the pump  $\alpha_+$ , is tightly phase locked to the cavity. Any phase variation of  $\alpha_+$  is translated by the servo loop into a phase correction fed back to the incoupled laser  $\alpha_+^{(in)}$ , thus suppressing any relative phase dynamics. Being interested mainly in the situation of one-sided pumping of the cavity ( $\eta_- = 0$ ), we also neglect variations of  $\alpha_+$  due to photon scattering from and into the (almost) empty probe  $\alpha_-$ . We then obtain a stationary field amplitude  $\alpha_+ = \chi^{-1}\eta_+$ , where we introduced the abbreviation  $\chi = \kappa + iNU_0 - i\Delta_c$ . Here  $N$  is the atom number,  $U_0$  the one-photon light shift, and  $\Delta_c$  the detuning of the laser from the resonance of the empty cavity. The very large detuning from the atomic resonances allows us to neglect the radiation pressure exerted by the cavity fields. The backscattered probe and the motions of the atoms located at the positions  $x_n$  are then described by

$$\begin{aligned} \dot{\alpha}_- &= -\chi\alpha_- - \frac{iU_0\eta_+}{\chi} \sum_n e^{2ikx_n}, \\ k\ddot{x}_n &= 2\varepsilon iU_0\eta_+ \left( \frac{\alpha_-}{\chi^*} e^{-2ikx_n} - \frac{\alpha_-^*}{\chi} e^{2ikx_n} \right) - \gamma_{\text{fric}} k\dot{x}_n, \end{aligned} \quad (1)$$

where  $k$  is the wave number of the field and  $\varepsilon \equiv \hbar k^2/m$  is twice the recoil shift. Note that we have phenomenologically included a damping term  $\gamma_{\text{fric}}kv$  to account for molasses friction. This procedure has been introduced in Ref. [13] to model the impact of atomic collisions. In our experiment, collisions are negligible.

In general the equations cannot be solved analytically, and we have to numerically iterate them. For the sake of computational efficiency we treat groups of  $10^4$  atoms as single particles. Figures 2(b) and 3(b) trace the simulated evolution of the coupled system consisting of the atomic cloud and two optical modes of the ring cavity as pump and probe. We find good agreement with the experimental data. The simulations also reveal that part of the atoms copropagate with the moving standing wave potential, sitting on its back slope and thus experiencing a constant accelerating light force. This force comes from the photonic momentum transfer accompanying the light scattering into the reverse mode: The atoms behave like surfing on a self-sustained standing light wave. Without friction the atoms continuously accelerate, and the standing wave ratio and the atomic bunching gradually decrease. The

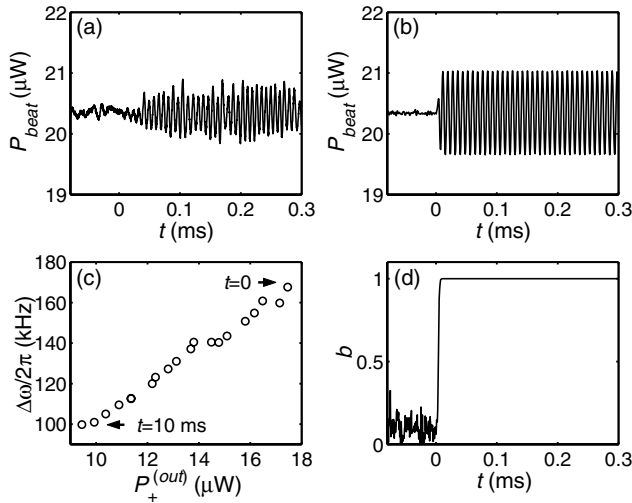


FIG. 3. (a) Formation of a moving standing wave upon irradiation of molasses beams at time  $t = 0$ . The experimental settings are the same as in Fig. 2(a) except for the light power  $P_+^{\text{cav}} = 11$  W. (b) Numerical simulation of the beat signal obtained with a unidirectionally pumped cavity ( $\eta_- = 0$ ) according to Eq. (1). The atom number and the friction coefficient are adjusted to  $N = 2 \times 10^5$  and  $\gamma_{\text{fric}} = 9\kappa$ , respectively. (d) The simulation also yields the bunching parameter  $b \equiv N^{-1} |\sum_n e^{2ikx_n}|$  defined in Ref. [5]. The perfect bunching for  $t > 0$  is an artifact of our simplified friction model, which does not account for diffusion heating by the molasses. (c) Impact of the pump rate  $\eta_+$  on the steady-state propagation velocity of the standing wave. The pump rate is ramped down within 10 ms and monitored through the outcoupled laser power  $P_+^{\text{(out)}}$ , which decreases from 18 to 10  $\mu\text{W}$ .

inclusion of friction leads to increased backscattering, deeper potential valleys, and stronger atomic bunching.

Analytic solutions can be derived for the case of perfect atomic bunching. We may then replace the atomic variables by center-of-mass coordinates  $x \equiv N^{-1} \sum_n x_n$ . Inserting the ansatz  $\alpha_- \equiv \beta e^{2ikx}$ , with the assumption of unidirectional pumping and steady-state conditions ( $\eta_- = 0$ ,  $\dot{\beta} = 0$ ), one obtains

$$\beta = \frac{-iNU_0\eta_+}{\chi(\chi + 2ikv)},$$

$$kv = \frac{4\epsilon NU_0^2\eta_+^2}{|\chi|^2} \text{Re}\left(\frac{1}{\chi + 2ikv}\right) - \gamma_{\text{fric}}kv. \quad (2)$$

For simplicity we assume  $\Delta_c = NU_0$ , which is generally satisfied when the laser is locked to the cavity, whose resonance is shifted by the presence of atoms [16]. Ignoring friction ( $\gamma_{\text{fric}} = 0$ ) and with the initial condition  $v(t = 0) = 0$ , the differential equation in (2) is solved by

$$(kv)^3 + \frac{3\kappa^2}{4}kv = \frac{3\epsilon NU_0^2\eta_+^2}{\kappa}t. \quad (3)$$

The analytic solution of this cubic equation is shown as a solid line in Fig. 2(c). In order to account for atomic

debunching, which is particularly strong during the one-sided switch-off procedure, we have assumed that only 1/10 of the atoms participate in the CARL process. In contrast, the introduction of friction to the dynamics leads to a steady state. At long times, where  $2kv \gg \kappa$ , the differential equation in (2) is approximately solved by

$$(kv)^3 = \frac{\epsilon NU_0^2\eta_+^2}{\kappa\gamma_{\text{fric}}}. \quad (4)$$

In summary, we studied the mutual backaction between the light field of a unidirectionally pumped high- $Q$  ring cavity and cold atoms trapped in this light field. For the first time, as far as we know, strong evidence for the central role played by bunching and by atomic recoil has been found: the former by observing a back-scattered probe field in the absence of a seed and the latter by detecting a displacement of the atomic sample. By introducing an optical molasses the system approaches a steady state, which might be interpreted as a cw CARL. The atomic self-bunching triggered by the molasses is an example for a phenomenon occurring in extended dynamical systems: the enhancement or even the seeding of spatiotemporal instabilities by a dissipative force.

We are grateful for helpful discussions with Helmut Ritsch. We acknowledge financial support from the Landesstiftung Baden-Württemberg.

- 
- [1] O. R. Frisch, *Z. Phys.* **86**, 42 (1933).
  - [2] J. Guo, P. R. Berman, H. Dubetsky, and G. Grynberg, *Phys. Rev. A* **46**, 1426 (1992).
  - [3] J. Y. Courtois, G. Grynberg, B. Lounis, and P. Verkerk, *Phys. Rev. Lett.* **72**, 3017 (1994).
  - [4] D. Kruse *et al.*, *Phys. Rev. A* **67**, 051802(R) (2003).
  - [5] R. Bonifacio and L. de Salvo, *Nucl. Instrum. Methods Phys. Res., Sect. A* **341**, 360 (1994); R. Bonifacio, L. DeSalvo, L. M. Narducci, and E. J. Dangelo, *Phys. Rev. A* **50**, 1716 (1994).
  - [6] P. R. Berman, *Phys. Rev. A* **59**, 585 (1999).
  - [7] R. Bonifacio and L. de Salvo, *Appl. Phys. B* **60**, S233 (1995).
  - [8] G. L. Lippi, G. P. Barozzi, S. Barbay, and J. R. Tredicce, *Phys. Rev. Lett.* **76**, 2452 (1996).
  - [9] P. R. Hemmer *et al.*, *Phys. Rev. Lett.* **77**, 1468 (1996).
  - [10] W. J. Brown, J. R. Gardner, D. J. Gauthier, and R. Vilaseca, *Phys. Rev. A* **56**, 3255 (1997).
  - [11] M. Gangl and H. Ritsch, *Phys. Rev. A* **61**, 043405 (2000).
  - [12] M. Perrin, G. L. Lippi, and A. Politi, *J. Mod. Opt.* **49**, 419 (2002).
  - [13] R. Bonifacio and P. Verkerk, *Opt. Commun.* **124**, 469 (1996).
  - [14] M. Perrin, G. L. Lippi, and A. Politi, *Phys. Rev. Lett.* **86**, 4520 (2002).
  - [15] M. Perrin, Zongxiong Ye, and L. Narducci, *Phys. Rev. A* **66**, 043809 (2002).
  - [16] Th. Elsässer, B. Nagorny, and A. Hemmerich, *Phys. Rev. A* **67**, 051401(R) (2003).